



Modeling the effects of tropospheric ozone on wheat growth and yield

Jose Rafael Guarin^{a,*}, Belay Kassie^b, Alsayed M. Mashaheet^{c,d}, Kent Burkey^e, Senthod Asseng^a

^a Department of Agricultural and Biological Engineering, University of Florida, Gainesville, FL, 32611, USA

^b Research and Development Division, DuPont Pioneer, 7000 NW 62nd Avenue, Johnston, IA, 50131, USA

^c Department of Entomology and Plant Pathology, North Carolina State University, Raleigh, NC, 27695, USA

^d Department of Plant Pathology, Faculty of Agriculture, Damanhour University, Damanhour, 22511, Egypt

^e Plant Science Research Unit, USDA-ARS, Raleigh, NC, 27607, USA



ARTICLE INFO

Keywords:

Ozone
Crop model
Wheat yield
Food security
Water stress
Elevated CO₂

ABSTRACT

Elevated tropospheric ozone (O₃) concentrations can negatively impact wheat growth by reducing photosynthesis and accelerating leaf senescence. Future global O₃ concentrations are expected to increase in many regions, which will further limit global wheat production. However, few crop models consider the effects of O₃ stress on wheat. We incorporated the effects of O₃ stress on photosynthesis and leaf senescence into the DSSAT-NWheat crop model and reproduced an observed experiment and reported yield declines from the literature. Simulated wheat yields decreased as daily O₃ concentrations increased above 25 ppb, with yield losses ranging from 0.26% to 0.95% per ppb O₃ increase, depending on the cultivar O₃ sensitivity. The model reproduced known wheat physiological responses from the combination of O₃ stress with water deficit and elevated atmospheric CO₂ concentration. Increased water deficit stress and elevated atmospheric CO₂ both reduce the negative impact of O₃, but yield benefits from elevated CO₂ can be lost due to elevated O₃ concentrations. The O₃-modified NWheat model simulates the effects of O₃ stress on wheat growth and yield in interaction with other growth factors and can be used for studies on climate change and O₃ impacts.

1. Introduction

Tropospheric or surface ozone (O₃) is a secondary pollutant created from photochemical reactions between incoming solar radiation and primary pollutants such as nitrogen oxides (NO_x = NO + NO₂), volatile organic compounds (VOCs), carbon monoxide (CO), or methane (CH₄), occurring in all areas of the globe (U.S. EPA, 2006; Simpson et al., 2014). Elevated concentrations of O₃ cause deleterious effects on crop growth and development (Mills et al., 2007; Leisner and Ainsworth, 2012), and future climate projections indicate increases in global O₃ concentrations (Vingarzan, 2004; Meehl et al., 2007; Wild et al., 2012). The risk of O₃ injury in global vegetation is projected to increase by 70% from 2000 to 2100 under the Intergovernmental Panel on Climate Change (IPCC) Representative Concentration Pathway 8.5, which is the highest emission scenario (Sicard et al., 2017). The largest increases of O₃ concentrations are expected in the tropics and subtropics due to projected growth of O₃ precursor emissions, especially in Southeast Asia, India, and Central America (Wild et al., 2012; Cooper et al., 2014). However, these increases in O₃ concentrations are not localized due to transportation of air pollutants across the lower atmosphere. For example, O₃ concentrations in remote regions in the Southern

Hemisphere are projected to increase in the future due to O₃ transport from source regions (Hauglustaine et al., 2005; Meehl et al., 2007).

The increasing trends of global atmospheric carbon dioxide (CO₂) and temperature suggest a significant change in the climate and future changes are inevitable regardless of efforts to reduce global emissions scenarios (IPCC, 2013). Climate change and extreme weather events cause abnormal variations in abiotic stress factors that affect crops (e.g., temperature, water, radiation, nutrient limitation, or pollutants) (Sheffield and Wood, 2008; Wehner et al., 2011). These changes and variations in climate can directly affect O₃ concentrations. O₃ concentrations are predicted to continue to rise across most of the world, and by 2030 elevated O₃ levels could pose a large threat to global food security (Fowler et al., 2008). O₃ concentrations are usually highest in the summer months, and climate change may extend the summer conditions in many locations, resulting in a drier and warmer fall. The prolonged summer conditions will increase O₃ concentrations in the fall due to a longer period of more active photochemical reactions (Battisti and Naylor, 2009; Zhang and Wang, 2016). In addition, heat waves may also increase the probability of extreme O₃ concentration events (Hou and Wu, 2016), and heat waves will become more frequent in the future (Semenov and Shewry, 2011; Trnka et al., 2014). Thus, future climate

* Corresponding author.

E-mail address: jguarin@ufl.edu (J.R. Guarin).

<https://doi.org/10.1016/j.eja.2019.02.004>

Received 6 June 2018; Received in revised form 13 December 2018; Accepted 5 February 2019

Available online 13 February 2019

1161-0301/ © 2019 Elsevier B.V. All rights reserved.

change and elevated O₃ concentrations will affect agricultural areas across the globe and should be considered when developing agricultural adaptation strategies.

Bread wheat (*Triticum aestivum* L.) is the second highest produced and most harvested crop in the world (FAOSTAT, 2017). Wheat contributes approximately 20% of the total global dietary calories and proteins and is the crop most consumed directly as food (Shiferaw et al., 2013). Global wheat production is negatively affected by abiotic stress factors, including O₃. Elevated O₃ concentrations reduce crop photosynthetic activity and accelerate leaf senescence due to cellular membrane destabilization and dysfunction. Elevated O₃ concentrations are especially damaging during the reproductive stage of growth because of increased abiotic stress sensitivity and high demand of resources for seed development (Feng et al., 2008; Leisner and Ainsworth, 2012). O₃ enters the crop through the leaf stomata and rapidly reacts with molecules in the intercellular air space to produce Reactive Oxygen Species (ROS) in the apoplast (e.g., hydrogen peroxide, singlet oxygen, superoxide radicals, hydroxyl radicals, and nitric oxide) (Nie et al., 1993; Langebartels et al., 2002; Ainsworth, 2017). The production of ROS in the apoplast triggers costly metabolic defense mechanisms and programmed cell death, which divert resources from growth and seed production and promote leaf senescence (Ainsworth, 2017). Both chronic and acute O₃ exposure reduce carboxylation capacity and increase production of the internal toxicant ethylene, often leading to chlorosis (Farage et al., 1991; Farage and Long, 1999; Vainonen and Kangasjarvi, 2015). The cellular response mechanism to O₃ varies among wheat cultivars, so it is important to know the O₃ response and sensitivity of the cultivar being studied (Feng et al., 2010).

In the field, abiotic stresses commonly occur simultaneously and interact with each other, and one stress can alter a crop's resistance to another stress. This results in compound effects and distinct crop responses (Tester and Bacic, 2005; Mittler, 2006). For example, studies in wheat have shown that water deficit stress may limit O₃ stress because water deficit causes stomatal closure to prevent water loss, which also reduces stomatal uptake of O₃ (Khan and Soja, 2003; Biswas and Jiang, 2011). Conversely, expanding irrigation into dryland agriculture will increase stomatal conductance (Roche, 2015), and increased stomatal conductance will enhance the uptake of O₃, increasing the negative impact from O₃ on crop growth (Khan and Soja, 2003). Thus, studies must consider the combined effects of stresses when developing adaptation strategies for wheat production.

Various global experiments have been conducted to determine the effects of O₃ stress on wheat production. Large-scale experimental field studies from the National Crop Loss Assessment Network (NCLAN) of the United States in the 1980s showed that wheat yield losses in the US ranged from 7% to 33% due to ambient O₃ concentrations (Heck et al., 1984; Heagle, 1989). The European Open Top Chamber (EOTC) program field experiments conducted in the early 1990s indicated that wheat yields in the European Union were reduced by 5% due to accumulated O₃ exposure above a 40 parts-per-billion (ppb) threshold (AOT40) (Mauzerall and Wang, 2001). A winter wheat fumigation experiment in the UK compared daily 7-hour (9:00–15:59 h) mean (M7) O₃ concentrations of 30 ppb and 80 ppb and found a 13% decrease in yield due to increased O₃ (Ollerenshaw and Lyons, 1999). A high altitude O₃ experiment at 900 m found that ambient levels of O₃ in 1989 and 1990 (M7 O₃ of 74 ppb and 90 ppb) reduced wheat yield by 9.6% and 11.6%, respectively, compared to carbon-filtered treatments (M7 O₃ of 36 ppb and 34 ppb) (Fuhrer et al., 1992). Wang and Mauzerall (2004) showed that wheat yields in China, Japan, and South Korea were reduced by 1% to 9% from M7 O₃ concentrations in 1990, and projected elevated O₃ concentrations in these countries will reduce wheat yield by 2% to 16% by 2020. In a study that examined and compared 19 major agricultural crops, wheat was found to be the most sensitive crop to O₃ exposure (Mills et al., 2007). A meta-analysis study found that when M7 O₃ concentration ranged between 31 ppb to 59 ppb (an average of 43 ppb), wheat yield was reduced by 18% and biomass

was reduced by 16% compared to 26 ppb (carbon-filtered O₃ concentration) (Feng et al., 2008). A follow-up meta-analysis study assessed the effects of elevated O₃ on wheat relative to a 26 ppb concentration and found that ambient M7 O₃ concentrations (31–50 ppb) reduced wheat yield by 9.7%, and future projected M7 O₃ concentrations (51–75 ppb) further decreased yield by an additional 10% (Feng and Kobayashi, 2009). Several studies analyzed the response of global wheat yield to exposure of seasonal daytime M7 O₃ and AOT40 in the year 2000 and found that O₃ pollution reduced global wheat yield by 3.9% to 15% (Van Dingenen et al., 2009; Avnery et al., 2011a). Additionally, future global wheat yield losses from O₃ were projected to range between 5.4% to 25.8% by 2030, with the highest losses ranging from 11.2% to 44.4% in South Asia (Avnery et al., 2011b). A recent study compared the impact of O₃ on wheat yield from non-filtered M7 O₃ concentrations to carbon-filtered M7 O₃ concentrations (mean of 35.6 ppb and 13.7 ppb, respectively) and found an average yield loss of 8.4%, or 0.38% yield loss per ppb O₃ increase (Pleijel et al., 2018).

Despite many studies highlighting the negative effects of O₃ on wheat production, few wheat crop simulation models consider the impacts of O₃ stress on wheat growth and development (Lobell and Gourdji, 2012; Lobell and Asseng, 2017). Ewert et al. (1999) modified the AFRCWHEAT (Porter, 1993) model and the LINTUL model (Spitters and Schapendonk, 1990) to include the effects of O₃ stress. Recently, the WOFOST crop model and the MCWLA-Wheat eco-physiological model were modified to account for O₃ stress (Capelli et al., 2016; Tao et al., 2017). Crop simulation models are widely applied in quantitative analysis of crop growth and cropping systems, and models that consider O₃ impacts on wheat growth and production could assist to mitigate future wheat yield loss.

This study aims to incorporate O₃ effect algorithms with a crop modeling approach to simulate the response of wheat growth and yield to current and elevated O₃ concentrations using the Decision Support System for Agrotechnology Transfer (DSSAT) wheat model, DSSAT-NWheat v.4.6.1.01. DSSAT is a crop modeling platform that combines models of various crops with software that facilitates evaluation and application of crop models for various objectives (Jones et al., 2003). DSSAT-NWheat is a well-known and widely used model that was validated with controlled field experiments and various agronomic treatments at many global locations (Kassie et al., 2016; Liu et al., 2016). NWheat was originally validated as part of the Agricultural Production Systems Simulator (APSIM) framework (Asseng et al., 1998, 2000, 2004). NWheat performed well when simulating nitrogen (N) dynamics and high heat effects in wheat growth compared to other crop models (Asseng et al., 2015), and the incorporation of O₃ effects will further improve simulations of real-world crop interactions.

2. Materials and methods

2.1. Model description

A new function for the effect of O₃ stress on wheat growth and development was added to the existing DSSAT-NWheat model. The NWheat model simulates wheat development and growth, water and N dynamics, and various stress factors and responses in daily time steps (Keating et al., 2001; Asseng et al., 2004). NWheat captures the effect of elevated atmospheric CO₂ concentrations on crop growth, radiation-use efficiency (RUE), and transpiration efficiency (TE) based on a RUE-CO₂-temperature function and a CO₂-TE function (Reyenga et al., 1999). NWheat uses two different subroutines to calculate the effects of abiotic stresses to reduce photosynthesis and accelerate leaf senescence since these processes affect the crop growth at different rates depending on the duration and severity of the stress. The O₃ stress function was incorporated into NWheat by modifying the photosynthesis reduction and leaf senescence acceleration subroutines so that the RUE-CO₂-temperature and the RUE-water functions and stress reduction factors interact with the effects of O₃.

2.2. Model effects of O_3 on photosynthesis and leaf senescence

The new function for the effect of O_3 stress in NWheat includes the two main responses of O_3 stress via stomatal uptake directly affecting photosynthesis and via accelerated leaf senescence (which also indirectly impacts photosynthesis). These two responses have different impact rates and can be influenced by other growing conditions, e.g. stomatal closure due to water stress or elevated atmospheric CO_2 reducing the direct O_3 impact on photosynthesis at a different rate than leaf senescence. The photosynthetic reduction effect of O_3 stress was incorporated into the model based on the existing approach in the NWheat model for abiotic stresses (Asseng et al., 2000; Keating et al., 2001), while also considering the interactive effects of O_3 concentrations with water deficit stress and elevated atmospheric CO_2 concentrations. The effect of O_3 stress accelerating leaf senescence was incorporated into the model similar to heat stress in which leaf senescence is accelerated above a set threshold (Asseng et al., 2011). Linear relationships were assumed for simplicity due to lack of detailed data.

The M7 O_3 concentration was chosen as the input into the model because the M7 exposure index is the most commonly used O_3 index (Ashmore, 2005). The M7 index was previously used in many other experimental and modeling studies that evaluated the effects of O_3 stress on wheat yield (Heck et al., 1984; Heagle, 1989; Lesser et al., 1990; Fuhrer et al., 1992; Wang and Mauzerall, 2004; Feng and Kobayashi, 2009; Avnery et al., 2011a, b). However, some studies also used other daily O_3 exposure indices to determine the effects of O_3 stress on wheat, such as AOT40, SUM06, and W126, but these indices put little emphasis on O_3 concentrations < 40 ppb, which can still damage crops (Ashmore, 2005; Mills et al., 2011a; Hollaway et al., 2012). Similar to the M7 index, the POD_Y (Phytotoxic O_3 Dose) effective flux accounts for the effects of lower O_3 concentrations, but it is not as commonly used as the M7 index (Mills et al., 2011b). Although M7 may lessen the effect of peak daytime O_3 concentrations since it is an average, studies have shown that hourly mean O_3 indices are a better estimator of O_3 damage to crops than hourly maximum O_3 indices (Heck et al., 1984).

A minimum O_3 stress threshold of 25 ppb was set based on pre-industrial O_3 concentrations and previous NCLAN studies, indicating O_3 damage usually occurs above this base threshold (Heck et al., 1984; Lesser et al., 1990; Feng and Kobayashi, 2009). When the O_3 concentration is above the set 25 ppb threshold, photosynthesis will be reduced by a factor between 0–1 (Eq. (1), Fig. 1a) and leaf senescence will be accelerated by a factor > 1 (Eq. (4), Fig. 1b).

Eq. (1) shows the photosynthesis reduction factor due to O_3 stress (FO_3) without interaction with water deficit stress and elevated atmospheric CO_2 :

$$FO_3 = -FOZ_1 * OZONX + FOZ_2 \quad (1)$$

where $OZONX$ refers to the daily M7 O_3 concentration in ppb and the parameter values, FOZ_1 and FOZ_2 (Table 1), are calibrated for the different O_3 sensitivities of wheat cultivars (see Fig. 1a and Section 2.3).

The FO_3 is further modified in Eq. (2) to include the interactions of O_3 stress with elevated atmospheric CO_2 concentration and water deficit stress ($PRFO_3$):

$$PRFO_3 = \min \left(1.0, \frac{FO_3 * rue_{factor}}{swdef(photo_{nw})} \right) \quad (2)$$

where FO_3 is the photosynthetic O_3 reduction factor without interaction with water deficit stress and elevated atmospheric CO_2 (Eq. (1)), rue_{factor} is the CO_2 effect > 350 ppm on potential dry matter (carbohydrate) production, and $swdef(photo_{nw})$ is the water deficit effect on photosynthesis based on the fraction of extractable soil water (Keating et al., 2001).

The dry matter production stress in the crop model is based on the limiting photosynthesis stress factors (Eq. (3)):

$$optfr = \min(swdef(photo_{nw}), nfact(1), PRFO_3 * prft) \quad (3)$$

where $optfr$ is the reduction of photosynthesis due to growth stresses (0–1) to be multiplied with the daily carbohydrate production to reduce dry matter accumulation, $swdef(photo_{nw})$ is the water deficit effect on photosynthesis, $nfact(1)$ is the nitrogen stress factor, $PRFO_3$ is the total O_3 stress factor accounting for water and CO_2 interactions (Eq. (2)), and $prft$ is the temperature stress factor.

Eq. (4) shows the leaf senescence acceleration factor due to O_3 stress ($SLFO_3$):

$$SLFO_3 = SLFOZ_1 * OZONX + SLFOZ_2 \quad (4)$$

where $OZONX$ refers to the daily M7 O_3 concentration in ppb and the parameter values, $SLFOZ_1$ and $SLFOZ_2$ (Table 1), are calibrated for the different O_3 sensitivities of wheat cultivars (Section 2.3). The $SLFO_3$ is multiplied with normal leaf senescence to accelerate total senescence (Eq. (5)):

$$leafsen = slan * sfactor * SLFO_3 \quad (5)$$

where $leafsen$ is daily total leaf senescence, $slan$ is the normal leaf senescence based on growth stages after emergence, $sfactor$ is the leaf senescence due to abiotic stresses (i.e., temperature and water), and $SLFO_3$ is the leaf senescence acceleration factor due to O_3 stress. Fig. 1b shows the $SLFO_3$ for different O_3 sensitivities of wheat cultivars. Table 1 displays the FO_3 and $SLFO_3$ equations calibrated for the different O_3 sensitivities of wheat cultivars.

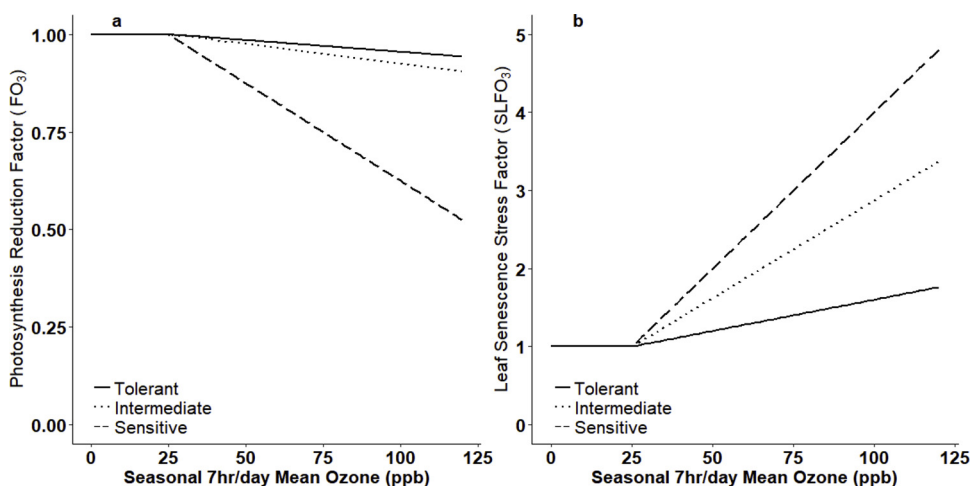


Fig. 1. NWheat functions for the (a) O_3 photosynthesis reduction factor without interaction with water deficit stress and elevated atmospheric CO_2 (FO_3) and (b) the O_3 leaf senescence acceleration stress factor ($SLFO_3$) for three different O_3 sensitive cultivar classifications applied to a crop grown at Maricopa, Arizona, USA (Kimball et al., 1999). Steeper slopes indicate a higher sensitivity to O_3 for both FO_3 and $SLFO_3$. Table 1 shows the equations for each cultivar classification of O_3 sensitivity.

Table 1

Summary of O_3 photosynthesis reduction factor without interaction with water deficit stress and elevated atmospheric CO_2 (FO_3) and O_3 leaf senescence acceleration stress factor ($SLFO_3$) equations for three different O_3 sensitive wheat cultivar classifications. $OZONX$ is daily M7 O_3 concentration (ppb) and parameter values are calibrated for each cultivar classification of O_3 sensitivity (Section 2.3).

Cultivar Classifications of O_3 Sensitivity	FO_3 (Eq. (1))	$SLFO_3$ (Eq. (4))
Tolerant	$FO_3 = -0.0006 * OZONX + 1.015$	$SLFO_3 = 0.008 * OZONX + 0.800$
Intermediate	$FO_3 = -0.0010 * OZONX + 1.025$	$SLFO_3 = 0.025 * OZONX + 0.375$
Sensitive	$FO_3 = -0.0050 * OZONX + 1.125$	$SLFO_3 = 0.040 * OZONX$

2.3. Calibration of O_3 equations

The added O_3 model equations were calibrated using simulations from an experiment without O_3 treatments conducted at Maricopa, Arizona, USA (33.06 °N, 111.98 °W, 361 m elevation) during the 1993–94 growing season (Hunsaker et al., 1996; Kimball et al., 1999, 2017). This experiment had no O_3 treatments, so it was used as a base for this simulation study. For the simulation, nine treatments were created consisting of constant daily O_3 concentrations of 25, 40, 50, 60, 70, 80, 90, 100, and 120 ppb for the entire growing season. The pre-industrial O_3 concentration of 25 ppb was considered as the control to evaluate the model with negligible effects of O_3 concentration (i.e., same output as simulation with 0 ppb O_3). The “Wet” treatment with ample N from Kimball et al. (1999) and a constant 350 ppm CO_2 concentration (base CO_2 in NWheat) were used to exclude any interactions between O_3 with water deficit, CO_2 , and N stress in this initial simulation experiment. The soil was a clay loam, Trix series (Table 2), and initial available soil water and N are described in Kimball et al. (1999). It was assumed that best management practices were used based on the “Wet” treatment, with scheduled sub-surface drip irrigation applications at 0.23 m depth throughout the season for a total of 629 mm from planting to harvest (Hunsaker et al., 1996). Cumulative rainfall from planting to harvest was 107 mm. The wheat cultivar used was Yecora Rojo planted on 13 December 1993 for all treatments. The simulation used fertilizer applications of urea via the irrigation system throughout the growing season for a total of 291 kg N/ha applied. Simulation start date was set six days before planting, and harvest date was set after crop maturity on 30 May 1994.

The observed data used for calibration were the predicted relative wheat yield losses from the Weibull model used in the NCLAN open-top field chamber study by Heck et al. (1984). The study examined four winter wheat cultivars (Abe, Arthur, Roland, and Vona) at four different seasonal M7 O_3 concentrations (40, 50, 60, and 90 ppb) and calculated the relative wheat yield loss to a base O_3 concentration of 25 ppb using the Weibull model. The Abe and Arthur cultivars were O_3 tolerant, while the Vona cultivar was considered O_3 sensitive. The Roland

cultivar O_3 sensitivity was between the sensitivity of the other cultivars, so its O_3 sensitivity was considered intermediate.

2.4. Observed O_3 exposure experiment

An air exclusion system (AES) field experiment was conducted in Wake County, North Carolina, USA (35.73 °N, 78.68 °W, 116 m elevation) from 17 November 2015 to 31 May 2016 to examine the effects of O_3 on winter wheat (cultivar Coker9553) growth using five different O_3 treatments with three replications each (15 plots in total). The O_3 treatments were ambient air (AA), carbon-filtered (CF), OZ-50, OZ-70, and OZ-90, where OZ- indicates added O_3 to ambient air with the number representing nominal 12-hour daytime average O_3 target concentration in ppb (hourly O_3 concentration was recorded, so M7 was calculated and used).

The plot layout for each treatment measured 8.2 m x 2.1 m. Panels consisting of a double layer of clear 10-mil PVC (vinyl) film were erected along the length of each side of the plot at a height of 1.1 m, and the short ends of the plot were open. The bottom half of the inner layer was perforated to allow conditioned air to be directed toward the base of the canopy, where it mixed with ambient air. Conditioned air was delivered to each panel by a fan box, providing an airflow of approximately 57 m³/min, totaling 114 m³/min for the entire plot.

The AA plots were open field plots with no surrounding structure, while all other plots were treated with conditioned air. To achieve the CF O_3 treatment, as ambient air moved through the fan box and passed through the initial particulate filter, the majority of the ambient O_3 was scrubbed from the air stream when passing through an activated carbon filter. To achieve the elevated O_3 treatments (OZ-50, OZ-70, and OZ-90), concentrated O_3 was injected into the conditioned air just downstream from the activated carbon filter. O_3 has a relatively short half-life (less than an hour), so it needed to be generated on site. All O_3 was produced from pure dry oxygen via corona cell discharge. A single generator (TG-20, Ozone Solutions) provided sufficient output to achieve the desired target O_3 concentration levels for the entire field. A custom program monitored and controlled the O_3 concentration in all

Table 2

Soil lower limit (LL), drained upper limit (DUL), and saturation (SAT) at various depths for the four US locations simulated. The soil series is specified below the name of each location.

Depth (cm)	Maricopa County, AZ Trix clay loam			Wake County, NC Appling sandy loam			Adams County, CO Weld loam			McLennan County, TX Lott silty clay		
	LL	DUL	SAT	LL	DUL	SAT	LL	DUL	SAT	LL	DUL	SAT
5	0.202	0.320	0.417	0.101	0.256	0.387	0.135	0.271	0.442	0.242	0.409	0.481
10	0.201	0.320	0.421	0.101	0.256	0.387	0.105	0.235	0.424	0.242	0.409	0.481
20	0.201	0.319	0.421	0.113	0.261	0.380	0.105	0.235	0.424	0.242	0.409	0.481
30	0.199	0.319	0.424	0.298	0.423	0.427	0.170	0.296	0.467	0.242	0.409	0.481
40	0.199	0.319	0.422	0.298	0.423	0.427	0.199	0.336	0.452	0.242	0.409	0.463
50	0.198	0.318	0.419	0.298	0.423	0.427	0.151	0.286	0.416	0.242	0.409	0.463
70	0.198	0.318	0.387	0.298	0.423	0.427	0.151	0.286	0.416	0.242	0.409	0.463
90	0.186	0.299	0.359	0.298	0.423	0.427	0.129	0.291	0.416	0.242	0.409	0.463
110	0.159	0.275	0.347	0.217	0.328	0.415	0.129	0.291	0.416	0.242	0.409	0.463
130	0.159	0.275	0.347	0.150	0.249	0.400	0.129	0.291	0.416	0.220	0.391	0.434
150	0.136	0.254	0.336	0.146	0.245	0.395	0.127	0.289	0.416	0.182	0.358	0.420
170	0.136	0.254	0.336	0.146	0.245	0.395	0.123	0.285	0.416	0.143	0.324	0.405
190	0.128	0.244	0.331	0.146	0.245	0.395	0.120	0.283	0.416	0.143	0.324	0.405
210	0.128	0.244	0.331	0.146	0.245	0.395	0.120	0.283	0.416	0.143	0.324	0.405

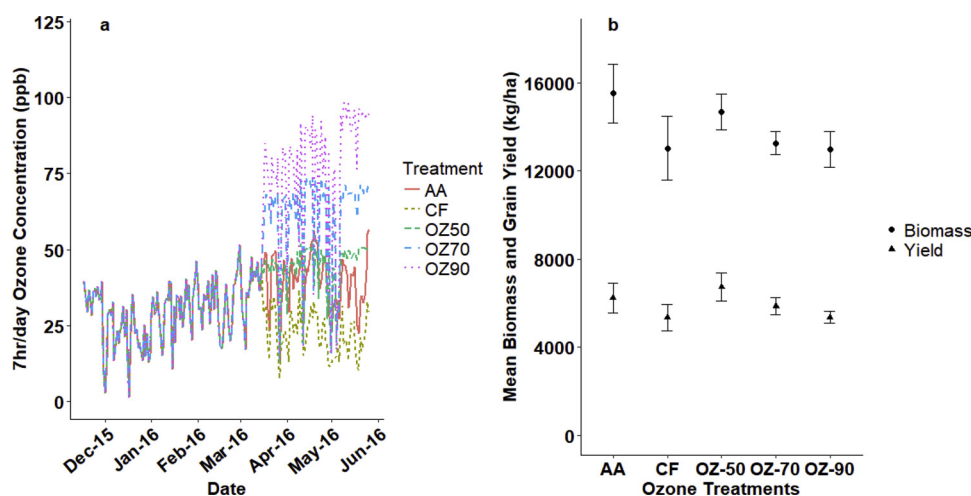


Fig. 2. (a) Mean observed daily M7 O₃ concentrations for the different O₃ treatments (i.e., mean of the three replications per treatment) from the Wake County, North Carolina, USA experiment and (b) the mean observed wheat, cultivar Coker9553, biomass (circles) and yield (triangles) for the O₃ treatments (i.e., mean of the three replications per treatment). Error bars indicate the standard error of the mean for the observed data.

plots using data from a commercial O₃ monitor (Model 49C, Thermo Fisher Scientific). O₃ target concentration levels were based on a 12-hour daytime diurnal profile, and a single mass flow controller (GFC17, Aalborg) was assigned to deliver concentrated O₃ to both fan boxes in a single plot through fluorinated ethylene propylene (FEP) tubing. O₃ dispensing only occurred during daylight hours, but O₃ measurements were recorded continuously throughout the season. O₃ sampling points were at canopy height at two positions centered along the length of each plot. All O₃ treatments received the same ambient O₃ concentrations from 17 November 2015 to 15 March 2016 measured hourly at 4 m above ground. From 16 March 2016 to 26 May 2016, O₃ was dispensed into the OZ- treatments and measured hourly at each plot. Fig. 2a shows the mean M7 O₃ concentrations of the replications for each O₃ treatment.

The wheat cultivar Coker9553 was planted on 17 November 2015. Applying sandy loam was the dominant soil series for the area of the experiment. Daily rainfall was measured on site (total of 728 mm from 1 November 2015 to 31 May 2016). Daily maximum and minimum air temperature were the same for all treatments from 1 November 2015 to 19 December 2015. From 20 December 2015 to 31 May 2016, maximum and minimum air temperatures and relative humidity were measured and recorded with sensors (HOBO U23, Onset Computer Corp.) at mid-canopy and full canopy heights centered along the length of each plot. Daily solar radiation at 2 m was collected from the State Climate Office of North Carolina, Climate Retrieval and Observations Network Of the Southeast (CRONOS) database for the experiment location from 1 November 2015 to 31 May 2016. All treatments received 17 drip irrigation applications between 5 April 2016 and 22 May 2016 for a total of 231 mm. One fertilizer application of phosphate, potash, ammonium nitrate, and gypsum (99 kg P/ha, 227 kg K/ha, 67 kg N/ha, and 124 kg Ca/ha, respectively) was applied on the day of planting with an additional application of ammonium nitrate (266 kg N/ha) on 3 March 2016 for all treatments. Fig. 2b shows the observed biomass and yield for each O₃ treatment.

Biomass and yield for the CF treatment (average M7 O₃ concentration of 26.9 ppb) were lower compared to the higher O₃ concentration treatments (average M7 O₃ concentration of 33.5, 35, 41.6, and 46.8 ppb for the AA, OZ-50, OZ-70, and OZ-90 treatments, respectively) from the O₃ exposure experiment (Fig. 2b). This disagrees with many previous O₃ exposure studies, although this phenomenon has been observed elsewhere (Flowers et al., 2007). Due to the high variation of biomass and yields within the observed data for each treatment, the AA treatment was selected for the relative comparison of biomass and yield loss instead of the CF treatment.

This Wake County, North Carolina O₃ response experiment was simulated with the NWheat model and compared with the observations. The cultivar Coker9553 was calibrated with the control AA treatment.

The Applying sandy loam soil parameters were from the United States Department of Agriculture (USDA) Natural Resources Conservation Service (NRCS) Web Soil Survey database (Soil Survey Staff, 2018) (Table 2). Based on the high observed yields, it was assumed that initial soil water availability was 100% and initial soil N content was 300 kg N/ha. Simulation start date was set on 1 November 2015.

2.5. Model sensitivity analysis of O₃ interaction with water deficit and CO₂

Two locations, Adams County, Colorado, USA (39.97°N, 104.4°W, 1520 m elevation) and McLennan County, Texas, USA (31.33°N, 97.35°W, 188 m elevation), were selected to study the simulated interactions of water deficit and CO₂ with O₃ stress. These areas were selected based on existing winter wheat production (USDA-NASS, 2017) and availability of hourly mean O₃ data. Daily weather data (e.g., precipitation and maximum and minimum temperature at 2 m) for each location was collected from the National Aeronautics and Space Administration (NASA) Prediction Of Worldwide Energy Resources (POWER) database on a 0.5° by 0.5° resolution (<http://power.larc.nasa.gov>). The daily solar radiation was calculated using the WeatherMan tool in DSSAT based on the means and variances of the precipitation and temperature data (Pickering et al., 1994). The hourly mean O₃ concentrations were from the National Oceanic and Atmospheric Administration (NOAA) Earth System Research Laboratory (ESRL) database from stations located at Erie, Boulder County, Colorado, USA (~48 km W of Adams County) from 2008 to 2015 and at Moody, McLennan County, Texas, USA from 2009 to 2013 (McClure-Begley et al., 2014). Any missing O₃ values were calculated using the monthly average O₃ for each hour. Fig. 3 shows the annual monthly O₃ concentrations averaged from the observed daily M7 O₃ concentrations for both locations. The soil profiles and depths for each location were obtained from the USDA NRCS Web Soil Survey database using the dominant soil series in each area (Soil Survey Staff, 2018) (Table 2).

The locations were set up in NWheat with eight treatments: rainfed with low CO₂, irrigated with low CO₂, rainfed with high CO₂, and irrigated with high CO₂, all with or without M7 O₃ concentrations. The low CO₂ treatments assumed a constant CO₂ concentration of 350 ppm to minimize effects from CO₂, and the high CO₂ concentration used a constant CO₂ concentration of 550 ppm. Based on the O₃ data available for the entire growing season, the harvest years simulated were from 2009 to 2016 at Adams County and from 2010 to 2013 at McLennan County. The above described weather and soil data were used, and best management practices were assumed. The rainfed treatments received no irrigation, and the irrigated treatments received automatic irrigation when the simulated extractable soil water fell below 100% so that the crop experienced no water deficit stress. Four fertilizer applications of ammonium nitrate (80 kg N/ha each) were applied at 0, 67, 125, and

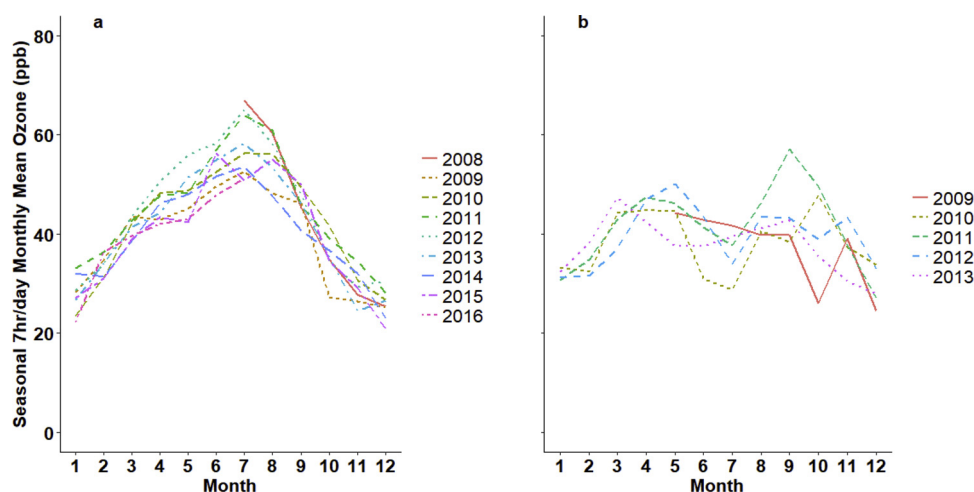


Fig. 3. Annual monthly O_3 concentrations averaged from the observed daily M7 O_3 concentrations for (a) Adams County, Colorado, USA and (b) McLennan County, Texas, USA.

167 days after planting to minimize N stress. Due to missing information on cultivars, the previously used winter wheat cultivar Coker9553 was planted each year on 20 September at Adams County and on 10 October at McLennan County, based on recent USDA planting recommendations for Colorado and Texas. Simulation start date was the first day of the planting month for each location and harvest date was automatically calculated based on when the model simulations reached maturity.

3. Results

3.1. Model calibration and validation

For calibration of the O_3 equations, the relative yield loss from observed data were compared to the relative yield loss from the model simulation. The simulated yield for the O_3 treatments > 25 ppb was divided by the control yield (i.e., 25 ppb treatment) to calculate the relative yield loss due to O_3 stress. The parameter values from Eqs. (1) and (4) were changed using the one-factor-at-a-time method (Morris, 1991) until the best fit was found for the relative yield loss of each of the different classifications of the O_3 sensitive cultivars (i.e., tolerant, intermediate, and sensitive). Fig. 4 illustrates the comparison between the observed relative yield loss and the simulated relative yield loss used for calibration of the three cultivar classifications of O_3 sensitivity at M7 O_3 concentrations ranging between 25 ppb to 120 ppb.

After the NWheat model was calibrated with the new O_3 equations,

the model was tested with data from other previous O_3 wheat studies. The simulated relative wheat yield losses from Fig. 4 (lines) were compared to additional observed relative wheat yield losses from other studies predicted using the Weibull model (Heck et al., 1983; Wang and Mauzerall, 2004) and a fitted linear model (Heck et al., 1982). The relative yield losses from the study by Wang and Mauzerall (2004) were based on the median Weibull parameters constructed from five wheat cultivars described by Lesser (1990). The relative yield losses from Heck et al. (1982) and Heck et al. (1983) were based on a linear model and the Weibull model, respectively, calculated from the combination of four NCLAN wheat cultivars (Blueboy II, Coker 47-27, Holly, and Oasis). Of the three simulated O_3 sensitive cultivar classifications tested, the tolerant O_3 cultivar classification provided the best fit to the additional observed relative wheat yield loss and was used for all simulations in this study (Table 3).

3.2. Sensitivity analysis of O_3 equations

A sensitivity analysis was conducted using the tolerant O_3 cultivar classification to check the model dynamics with the new O_3 impact equations. The Maricopa, Arizona, USA experiment was used again as the basis for the sensitivity analysis (Hunsaker et al., 1996; Kimball et al., 1999, 2017). Both the “Wet” and “Dry” treatments with ample N were used with additional O_3 levels applied in the simulation. The “Dry” treatment was similar to the above described “Wet” treatment, but with fewer scheduled drip irrigation applications throughout the

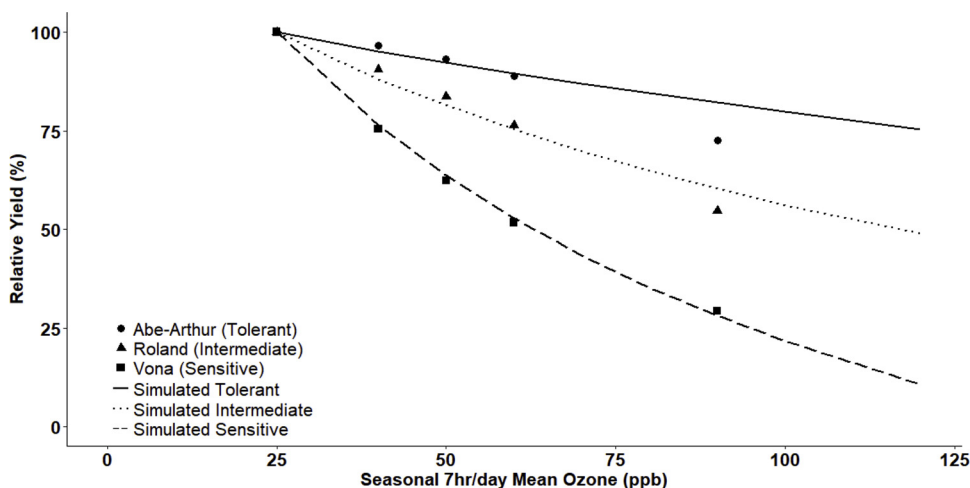


Fig. 4. NWheat model calibration. Observed relative yields (yield at seasonal M7 O_3 concentrations compared to yield at reference 25 ppb O_3 concentration) predicted from the Weibull function for O_3 sensitive wheat cultivars from Heck et al. (1984) (symbols) and simulated (lines) relative yields calibrated for each of the three O_3 sensitive wheat cultivars based on the Maricopa, Arizona, USA experiment.

Table 3

Normalized Root Mean Square Error (NRMSE) and coefficient of determination (R^2) calculated from the observed vs simulated relative yield loss (%) for the three O_3 sensitive cultivar classifications.

	Tolerant	Intermediate	Sensitive
NRMSE (%)	7	16	43
R^2	0.94	0.91	0.88

season for a total of 287 mm from planting to harvest to create higher water deficit stress (Hunsaker et al., 1996).

The O_3 treatments applied were the same treatments used for the model calibration (Section 2.3). Each new O_3 impact equation was tested individually. For example, when testing Eq. (1), Eq. (4) was set to one so that there was no accelerated leaf senescence effect and vice versa. Fig. 5 shows the simulated wheat yield using the different equations individually for the seasonal M7 O_3 concentrations for both “Wet” and “Dry” treatments.

It was expected that yield would decrease as M7 O_3 concentrations increased for all treatments and equations tested. However, the sensitivity analysis revealed that further analysis was warranted due to an increase of wheat yield as O_3 concentrations increased when using only the photosynthetic reduction equation for the “Dry” treatment (Fig. 5a). It was found that the reduced biomass growth from O_3 stress limited water uptake early in the season and demand later in the season, resulting in small yield increases under water stress conditions. This is illustrated in Fig. 6 showing the extractable soil water and cumulative water stress at different M7 O_3 concentrations for one of the photosynthetic reduction equations used in Fig. 5a (all equations from 5a had similar water dynamics). This effect of O_3 is similar to the findings from a study by Asseng and van Herwaarden (2003) in which N deficit reduced growth, water uptake, and demand, resulting in some cases of higher yields with less biomass growth in observations and simulations.

3.3. Simulated and observed relative yield loss for the observed AES O_3 exposure experiment

Fig. 7 shows the comparison between the observed and simulated biomass and yield loss relative to the AA treatment for each of the added O_3 treatments from the North Carolina field experiment. The simulated relative biomass and yield losses decreased as the seasonal M7 O_3 concentrations of each treatment increased above the AA treatment concentration, average of 33.5 ppb (average of 35, 41.6, and 46.8 ppb for the OZ-50, OZ-70, and OZ-90 treatments, respectively).

The observed relative biomass loss shows the same decreasing trend as O_3 concentrations increase, similar to the simulated relative yield loss but with higher biomass losses (Fig. 7a). The observed relative yield differed from the simulated trend as it increased under the OZ-50 treatment compared to the AA treatment and decreased under the OZ-70 and OZ-90 treatments (Fig. 7b). Table 4 shows the normalized root mean square error (i.e. root mean square error divided by the average of the observed dataset) from the statistical analysis between the observed versus simulated biomass and yield and relative biomass and yield losses used in Fig. 7.

3.4. Simulated relative yield loss due to combined interactions of O_3 , water deficit, and CO_2

Fig. 8 shows the simulated effects on wheat yield from the interaction of M7 O_3 concentrations with water deficit and elevated CO_2 at Adams County, Colorado from 2009 to 2016 and at McLennan County, Texas from 2010 to 2013. The inclusion of elevated O_3 in simulations reduced yield in all treatments but had varying severity. The irrigated treatments produced higher yields than the rainfed treatments at both locations, but the irrigated treatments with low CO_2 had the highest yield losses from O_3 stress. The irrigated treatments with high CO_2 had the lowest yield losses from O_3 stress. The rainfed treatment with low CO_2 had the lowest yields at both locations because of the increased water deficit stress throughout the growing season, especially in the warmer and drier climate of Texas.

4. Discussion

4.1. O_3 effect on simulated yields

The relative simulated wheat yield loss increases as the M7 O_3 concentrations increase above the 25 ppb threshold (Fig. 4). Using the O_3 tolerant cultivar classification, yield loss increased from 4.8% to 24.8% for the M7 O_3 concentrations increasing from 40 ppb to 120 ppb, an average yield loss of 0.26% per ppb M7 O_3 increase above 25 ppb. The average yield loss was 0.54% and 0.95% per ppb M7 O_3 increase above 25 ppb for the O_3 intermediate and O_3 sensitive cultivar classifications, respectively. These simulated yield loss per ppb averages agree with calculated yield losses in other studies. In these studies, Pleijel et al. (2018) reported an average yield loss of 0.38% per ppb O_3 increase, while Feng and Kobayashi (2009) reported an average yield loss of 0.67% per ppb O_3 increase. Feng et al. (2008) reported an average yield loss of 0.94% per ppb O_3 increase, Ollerenshaw and Lyons (1999) reported an average yield loss of 0.26% per ppb O_3 increase, and

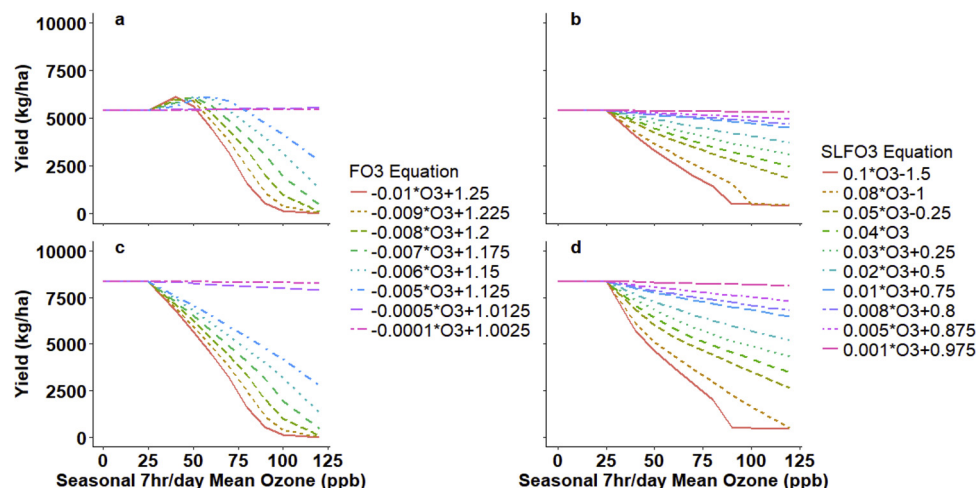


Fig. 5. Simulated wheat yield at various seasonal M7 O_3 concentrations from the sensitivity analysis of different O_3 photosynthesis reduction equations, FO₃ (a, c) and O_3 leaf senescence acceleration equations, SLFO₃ (b, d) for the Maricopa, Arizona, USA experiment “Dry” (a, b) and “Wet” (c, d) treatments.

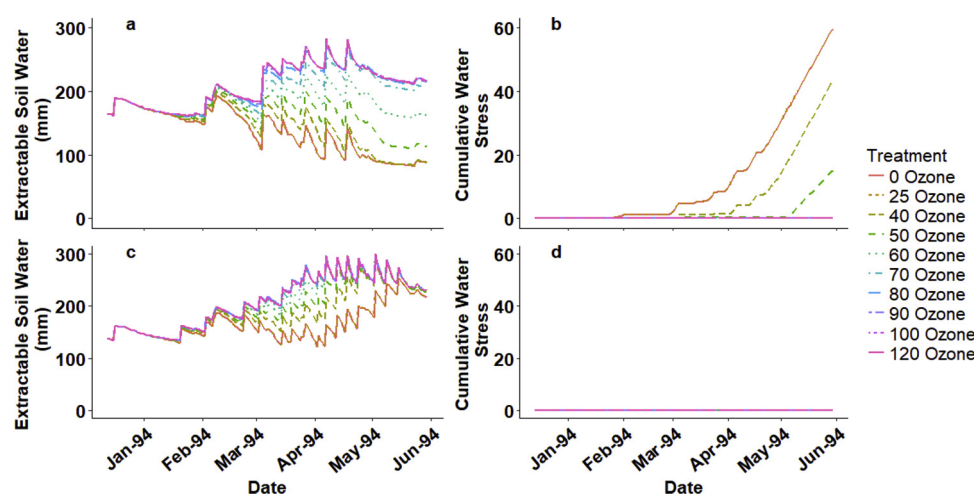


Fig. 6. Explanation for the yield increase in Fig. 5a using the example equation: $FO_3 = -0.01 \cdot O_3 + 1.25$. Simulated extractable soil water (a, c) and cumulative water stress (b, d) for the Maricopa, Arizona, USA experiment “Dry” (a, b) and “Wet” (c, d) treatments with additional different seasonal M7 O_3 concentrations (lines).

Fuhrer et al. (1992) reported an average yield loss of 0.23% per ppb O_3 increase. These studies covered different ranges of O_3 concentrations and the exact yield loss per ppb is not always constant over a large range of O_3 concentrations. The yield loss will depend on the O_3 sensitivity of the wheat cultivar as well as environmental interactions (Feng et al., 2010), with both factors considered in the NWheat model.

4.2. Uncertainty in the observed AES O_3 exposure experiment

All crop models contain uncertainty because they are simplifications of complex biological processes, but experimental data contain uncertainty as well. While the simulated relative biomass and yield loss trends agree with previous literature, where increasing O_3 concentrations decrease wheat dry matter and yield (Fowler et al., 2008; Feng and Kobayashi, 2009; Pleijel et al., 2018), the observed relative yield trend in the North Carolina experiment is unusual due to the yield increase from the AA treatment to a higher O_3 concentration treatment (OZ-50). The high standard error of the mean in the observed data (Fig. 7) caused an inflated NRMSE (Table 4) which indicates that the unusual observed relative yield trend might be due to large variation within each experimental treatment. This variation may be caused by different environmental growth conditions from the experimental AES plots compared to field conditions or the process of hormesis in which low levels of stress may actually benefit crop growth (Flowers et al.,

Table 4

Normalized Root Mean Square Error (NRMSE) calculated from the observed vs simulated biomass and yield and relative biomass and yield losses compared to the AA treatment (%) using the replications from the AES O_3 exposure experiment.

	Biomass	Yield	Relative Biomass to AA ^a	Relative Yield to AA ^a
NRMSE (%)	13	22	12	23

^a Ambient air treatment from the AES O_3 exposure experiment.

2007; Calabrese, 2014). Interestingly, the simulations also suggested small yield increases with low levels of O_3 concentrations under certain water limiting conditions, where reduced growth early in the season can preserve water for later in the season leading to small increases in yield (Fischer, 1979).

4.3. Combined effects of O_3 with water deficit and elevated CO_2

The simulated irrigated treatments with low CO_2 had the highest wheat yield loss from O_3 stress, agreeing with the findings from Khan and Soja (2003) that an abundant water supply increases impacts from O_3 stress. Additionally, the simulated irrigated treatments with high CO_2 had the lowest yield loss from O_3 , consistent with other studies in which elevated CO_2 mitigated some of the negative impacts of O_3 stress

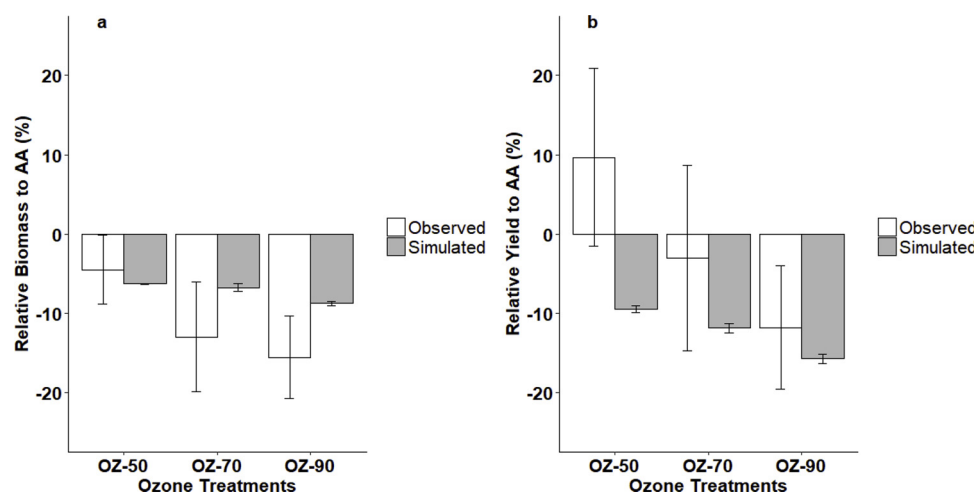


Fig. 7. Observed and simulated (a) relative biomass and (b) relative yield of O_3 concentration treatments to the ambient air (AA) treatment from the Wake County, North Carolina, USA O_3 exposure experiment. Error bars show standard error of the mean for the observed and simulated treatments.

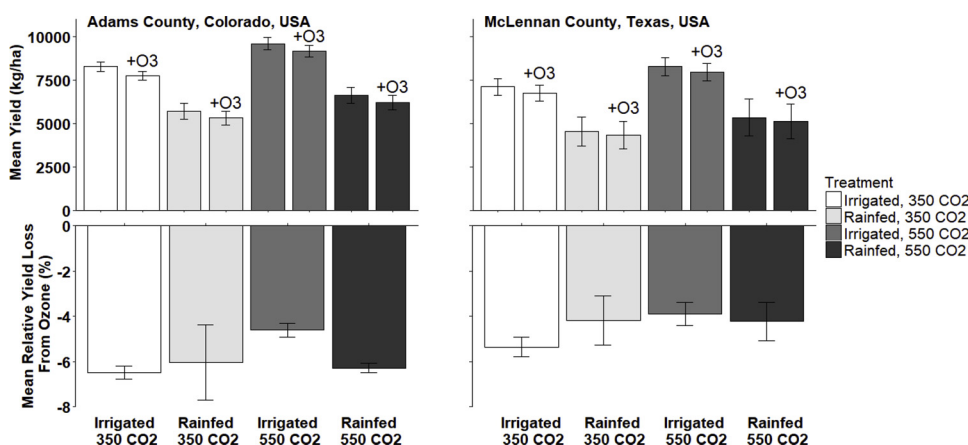


Fig. 8. Mean simulated yield and relative yield loss from 2009 to 2016 at Adams County, Colorado, USA (left) and from 2010 to 2013 at McLennan County, Texas, USA (right). Mean simulated yields with and without daily M7 O₃ concentrations (labeled) from Fig. 3 for rainfed with 350 ppm CO₂, irrigated with 350 ppm CO₂, rainfed with 550 ppm CO₂, and irrigated with 550 ppm CO₂ treatments (labeled). Error bars indicate standard error of the mean based on all years.

(Mauzerall and Wang, 2001; Ainsworth et al., 2008; Biswas et al., 2013).

The rainfed treatments with low CO₂ had the lowest simulated yields at both locations due to high water deficit stress. The rainfed treatments with low CO₂ also had a similar yield loss from O₃ stress as the rainfed treatments with high CO₂, which was unexpected. It was expected that the rainfed treatments with high CO₂ would have a lower yield loss from O₃ stress than the rainfed treatments with low CO₂. This discrepancy was explained in the year-to-year variation of simulated yields. The high variation in the simulated yield for the rainfed treatments was due to the high variability of rainfall for each year. The rainfall variability sometimes resulted in particularly high-simulated water deficit stress during the reproductive stage (e.g., 2011 simulation at Adams County, Colorado). Water deficit stress in 2011 during anthesis and grain filling was higher than in any of the other simulated years and resulted in the model simulating higher yields in the rainfed treatment with low CO₂ including O₃ stress than in the treatment without O₃ stress (3.35 and 3.17 t/ha, respectively). This was due to more available water later in the season from low biomass growth early in the season caused by O₃ stress (Section 3.2). Excluding 2011 resulted in the mean relative yield loss from O₃ for the rainfed treatment with low CO₂ increasing from -6.04% to -7.50%. The rainfed treatments with high CO₂ had lower O₃ effect on yield than the rainfed treatments with low CO₂ for the other simulated seasons, which was expected. Overall, the difference between the relative yield loss from O₃ for the rainfed treatments with low CO₂ and the rainfed treatments with high CO₂ was within 0.23%, which was explained by the rainfall variability.

5. Conclusion

The effects of O₃ stress were incorporated into the DSSAT-NWheat crop model by adding new functions reducing photosynthetic activity and accelerating leaf senescence. Model testing showed that simulated wheat yields responded similar to observed data and as expected in a sensitivity analysis. The O₃ impact on crop growth and yield depends on the scenario being studied when determining the effects of multiple abiotic stresses on crop responses. Each stress combination can cause distinct crop mechanisms that vary depending on stress severity, stress exposure, stress frequency, crop species and genotype (i.e., plasticity), and plant developmental stage (i.e., sensitivity).

The new addition of the O₃ stress functionality into the NWheat crop model reduces uncertainty by considering a new environmental growth factor in the model and will improve simulations of real-world environmental interactions. The O₃-modified NWheat model can be used to simulate the effects of O₃ stress on wheat growth in combination with climate change aspects. To further enhance model development and performance, the NWheat model should be tested with additional empirical data from O₃ exposure field experiments that focus

on the effects from O₃ stress and the interaction between O₃ and other stresses. It will also be beneficial to compare the O₃-modified NWheat model with other O₃-incorporated crop models. This will allow for improvements of future O₃ multi-model ensemble studies conducted by the AGMIP (Agricultural Model Intercomparison and Improvement Project; <http://www.agmip.org/>) modeling community.

Acknowledgements

The authors would like to thank Walter Pursley and Samuel Ray for field operations and data management associated with the AES field experiment conducted in Raleigh, NC. J.R.G. would like to thank the Florida Education Fund and the McKnight Doctoral Fellowship program for the support provided.

References

- Ainsworth, E.A., 2017. Understanding and improving global crop response to ozone pollution. *Plant J.* 90, 886–897.
- Ainsworth, E.A., Rogers, A., Leakey, A.D.B., 2008. Targets for crop biotechnology in a future high-CO₂ and high-O₃ world. *Plant Physiol.* 147, 13–19.
- Ashmore, M.R., 2005. Assessing the future global impacts of ozone on vegetation. *Plant Cell Environ.* 28, 949–964.
- Asseng, S., van Herwaarden, A.F., 2003. Analysis of the benefits to wheat yield from assimilates stored prior to grain filling in a range of environments. *Plant Soil* 256, 217–229.
- Asseng, S., Keating, B.A., Fillery, I.R.P., Gregory, P.J., Bowden, J.W., Turner, N.C., Palta, J.A., Abrecht, D.G., 1998. Performance of the APSIM-wheat model in Western Australia. *Field Crops Res.* 57, 163–179.
- Asseng, S., van Keulen, H., Stol, W., 2000. Performance and application of the APSIM NWheat model in the Netherlands. *Eur. J. Agron.* 12, 37–54.
- Asseng, S., Jamieson, P.D., Kimball, B., Pinter, P., Sayre, K., Bowden, J.W., Howden, S.M., 2004. Simulated wheat growth affected by rising temperature, increased water deficit and elevated atmospheric CO₂. *Field Crops Res.* 85, 85–102.
- Asseng, S., Foster, I., Turner, N.C., 2011. The impact of temperature variability on wheat yields. *Glob. Change Biol.* 17, 997–1012.
- Asseng, S., Ewert, F., Martre, P., Rotter, R.P., Lobell, D.B., Cammarano, D., Kimball, B.A., Ottman, M.J., Wall, G.W., White, J.W., Reynolds, M.P., Alderman, P.D., Prasad, P.V.V., Aggarwal, P.K., Anothai, J., Basso, B., Biernath, C., Challinor, A.J., De Sanctis, G., Doltra, J., Fereres, E., Garcia-Vile, M., Gayler, S., Hoogenboom, G., Hunt, L.A., Izaurralde, R.C., Jabloun, M., Jones, C.D., Kersebaum, K.C., Koehler, A.K., Muller, C., Kumar, S.N., Nendel, C., O'Leary, G., Olesen, J.E., Palosuo, T., Priesack, E., Rezaei, E.E., Ruane, A.C., Semenov, M.A., Shcherbak, I., Stockle, C., Stratonovitch, P., Streck, T., Supit, I., Tao, F., Thorburn, P.J., Waha, K., Wang, E., Wallach, D., Wolf, I., Zhao, Z., Zhu, Y., 2015. Rising temperatures reduce global wheat production. *Nat. Clim. Change* 5, 143–147.
- Avnery, S., Mauzerall, D.L., Liu, J.F., Horowitz, L.W., 2011a. Global crop yield reductions due to surface ozone exposure: 1. Year 2000 crop production losses and economic damage. *Atmos. Environ.* 45, 2284–2296.
- Avnery, S., Mauzerall, D.L., Liu, J.F., Horowitz, L.W., 2011b. Global crop yield reductions due to surface ozone exposure: 2. Year 2030 potential crop production losses and economic damage under two scenarios of O₃ pollution. *Atmos. Environ.* 45, 2297–2309.
- Battisti, D.S., Naylor, R.L., 2009. Historical warnings of future food insecurity with unprecedented seasonal heat. *Science* 323, 240–244.
- Biswas, D.K., Jiang, G.M., 2011. Differential drought-induced modulation of ozone tolerance in winter wheat species. *J. Exp. Bot.* 62, 4153–4162.
- Biswas, D.K., Xu, H., Li, Y.G., Ma, B.L., Jiang, G.M., 2013. Modification of photosynthesis

- and growth responses to elevated CO₂ by ozone in two cultivars of winter wheat with different years of release. *J. Exp. Bot.* 64, 1485–1496.
- Calabrese, E.J., 2014. Hormesis: a fundamental concept in biology. *Microb. Cell* 1, 145–149.
- Capelli, G., Confalonieri, R., Van Der Berg, M., Dentener, F., 2016. Modelling Inclusion, Testing and Benchmarking of the Impacts of Ozone Pollution on Crop Yields at Regional Level. Università Degli Studi Di Milano. Publications Office of the European Union, Luxembourg, pp. 1–61.
- Cooper, O.R., Parrish, D.D., Ziemke, J., Balashov, N.V., Cupeiro, M., Galbally, I.E., Gilge, S., Horowitz, L., Jensen, N.R., Lamarque, J.-F., Naik, V., Oltmans, S.J., Schwab, J., Shindell, D.T., Thompson, A.M., Thouret, V., Wang, Y., Zbinden, R.M., 2014. Global distribution and trends of tropospheric ozone: an observation-based review. *Elementa Sci. Anthropol.* 2.
- Ewert, F., van Oijen, M., Porter, J.R., 1999. Simulation of growth and development processes of spring wheat in response to CO₂ and ozone for different sites and years in Europe using mechanistic crop simulation models. *Eur. J. Agron.* 10, 231–247.
- FAOSTAT, 2017. Food and Agricultural Organization of the United Nations, FAOSTAT Statistics Database. FAO.
- Farage, P.K., Long, S.P., 1999. The effects of O₃ fumigation during leaf development on photosynthesis of wheat and pea: an in vivo analysis. *Photosyn. Res.* 59, 1–7.
- Farage, P.K., Long, S.P., Lechner, E.G., Baker, N.R., 1991. The sequence of change within the photosynthetic apparatus of wheat following short-term exposure to ozone. *Plant Physiol.* 95, 529–535.
- Feng, Z.Z., Kobayashi, K., 2009. Assessing the impacts of current and future concentrations of surface ozone on crop yield with meta-analysis. *Atmos. Environ.* 43, 1510–1519.
- Feng, Z.Z., Kobayashi, K., Ainsworth, E.A., 2008. Impact of elevated ozone concentration on growth, physiology, and yield of wheat (*Triticum aestivum* L.): a meta-analysis. *Glob. Change Biol.* 14, 2696–2708.
- Feng, Z.Z., Pang, J., Nouchi, I., Kobayashi, K., Yamakawa, T., Zhu, J.G., 2010. Apoplastic ascorbate contributes to the differential ozone sensitivity in two varieties of winter wheat under fully open-air field conditions. *Environ. Pollut.* 158, 3539–3545.
- Fischer, R.A., 1979. Growth and water limitation to dryland wheat yield in Australia: a physiological framework. *J. Aust. Inst. Agric. Sci.* 45, 83–94.
- Flowers, M.D., Fiscus, E.L., Burke, K.O., Booker, F.L., Dubois, J.J.B., 2007. Photosynthesis, chlorophyll fluorescence, and yield of snap bean (*Phaseolus vulgaris* L.) genotypes differing in sensitivity to ozone. *Environ. Exp. Bot.* 61, 190–198.
- Fowler, D., Amann, M., Anderson, R., Ashmore, M., Cox, P., Depledge, M., Derwent, D., Grennfelt, P., Hewitt, N., Hov, O., Jenkin, M., Kelly, F., Liss, P., Pilling, M., Pyle, J., Slingo, J., Stevenson, D., 2008. Ground-level Ozone in the 21st Century: Future Trends, Impacts and Policy Implications. Royal Society Policy Document 15/08. London, p. 132.
- Fuhrer, J., Grimm, A.G., Tschannen, W., Shariatmadari, H., 1992. The response of spring wheat (*Triticum aestivum* L.) to ozone at higher elevations 2. Changes in yield, yield components and grain quality in response to ozone flux. *New Phytol.* 121, 211–219.
- Hauglustaine, D.A., Lathiere, J., Szopa, S., Folberth, G.A., 2005. Future tropospheric ozone simulated with a climate-chemistry-biosphere model. *Geophys. Res. Lett.* 32, 5.
- Heagle, A.S., 1989. Ozone and crop yield. *Annu. Rev. Phytopathol.* 27, 397–423.
- Heck, W.W., Taylor, O.C., Adams, R., Bingham, G., Miller, J., Preston, E., Weinstein, L., 1982. Assessment of crop loss from ozone. *J. Air Pollut. Control Assoc.* 32, 353–361.
- Heck, W.W., Adams, R.M., Cure, W.W., Heagle, A.S., Heggstad, H.E., Kohut, R.J., Kress, L.W., Rawlings, J.O., Taylor, O.C., 1983. A reassessment of crop loss from ozone. *Environ. Sci. Technol.* 17, A572–A581.
- Heck, W.W., Cure, W.W., Rawlings, J.O., Zaragoza, L.J., Heagle, A.S., Heggstad, H.E., Kohut, R.J., Kress, L.W., Temple, P.J., 1984. Assessing impacts of ozone on agricultural crops: 2. Crop yield functions and alternative exposure statistics. *J. Air Pollut. Control Assoc.* 34, 810–817.
- Hollaway, M.J., Arnold, S.R., Challinor, A.J., Emberson, L.D., 2012. Intercontinental trans-boundary contributions to ozone-induced crop yield losses in the Northern Hemisphere. *Biogeosciences* 9, 271–292.
- Hou, P., Wu, S.L., 2016. Long-term changes in extreme air pollution meteorology and the implications for air quality. *Sci. Rep.* 6, 9.
- Hunsaker, D.J., Kimball, B.A., Pinter, P.J., LaMorte, R.L., Wall, G.W., 1996. Carbon dioxide enrichment and irrigation effects on wheat evapotranspiration and water use efficiency. *Trans. Asae* 39, 1345–1355.
- IPCC, 2013. Climate change 2013: the physical science basis. In: Stocker, T.F., Qin, D., Plattner, G.-K., Tignor, M., Allen, S.K., Boschung, J., Nauels, A., Xia, Y., Bex, V., Midgley, P.M. (Eds.), Contribution of Working Group I to the Fifth Assessment Report of the Intergovernmental Panel on Climate Change, pp. 1535 Cambridge, United Kingdom and New York, NY, USA.
- Jones, J.W., Hoogenboom, G., Porter, C.H., Boote, K.J., Batchelor, W.D., Hunt, L.A., Wilkens, P.W., Singh, U., Gijsman, A.J., Ritchie, J.T., 2003. The DSSAT cropping system model. *Eur. J. Agron.* 18, 235–265.
- Kassie, B.T., Asseng, S., Porter, C.H., Royce, F.S., 2016. Performance of DSSAT-Nwheat across a wide range of current and future growing conditions. *Eur. J. Agron.* 81, 27–36.
- Keating, B.A., Meinke, H., Probert, M.E., Huth, N.I., Hills, I.G., 2001. NWheat: documentation and performance of a wheat module for APSIM. *Trop. Agric. Tech. Memorandum* 1–66.
- Khan, S., Soja, G., 2003. Yield responses of wheat to ozone exposure as modified by drought-induced differences in ozone uptake. *Water Air Soil Pollut.* 147, 299–315.
- Kimball, B.A., LaMorte, R.L., Pinter, P.J., Wall, G.W., Hunsaker, D.J., Adamsen, F.J., Leavitt, S.W., Thompson, T.L., Matthias, A.D., Brooks, T.J., 1999. Free-air CO₂ enrichment and soil nitrogen effects on energy balance and evapotranspiration of wheat. *Water Resour. Res.* 35, 1179–1190.
- Kimball, B.A., Pinter Jr., P.J., LaMorte, R.L., Leavitt, S.W., Hunsaker, D.J., Wall, G.W., Wechsung, F., Wechsung, G., Bloom, A.J., White, J.W., 2017. Data from the Arizona FACE (free-air CO₂ enrichment) experiments on wheat at ample and limiting levels of water and nitrogen. *Open Data J. Agric. Res.* 3, 29–38.
- Langebartels, C., Wohlgenuth, H., Kschieschan, S., Grun, S., Sandermann, H., 2002. Oxidative burst and cell death in ozone-exposed plants. *Plant Physiol. Biochem.* 40, 567–575.
- Leisner, C.P., Ainsworth, E.A., 2012. Quantifying the effects of ozone on plant reproductive growth and development. *Glob. Change Biol.* 18, 606–616.
- Lesser, V.M., Rawlings, J.O., Spruill, S.E., Somerville, M.C., 1990. Ozone effects on agricultural crops: statistical methodologies and estimated dose-response relationships. *Crop Sci.* 30, 148–155.
- Liu, B., Asseng, S., Liu, L.L., Tang, L., Cao, W.X., Zhu, Y., 2016. Testing the responses of four wheat crop models to heat stress at anthesis and grain filling. *Glob. Change Biol.* 22, 1890–1903.
- Lobell, D.B., Asseng, S., 2017. Comparing estimates of climate change impacts from process-based and statistical crop models. *Environ. Res. Lett.* 12, 12.
- Lobell, D.B., Gourdji, S.M., 2012. The influence of climate change on global crop productivity. *Plant Physiol.* 160, 1686–1697.
- Mauzerall, D.L., Wang, X.P., 2001. Protecting agricultural crops from the effects of tropospheric ozone exposure: reconciling science and standard setting in the United States, Europe, and Asia. *Ann. Rev. Energy Environ.* 26, 237–268.
- McClure-Begley, A., Petropavlovskikh, I., Oltmans, S., 2014. NOAA Global Monitoring Surface Ozone Network. 1973–2014. National Oceanic and Atmospheric Administration, Earth Systems Research Laboratory Global Monitoring Division, Boulder, CO.
- Meehl, G.A., Stocker, T.F., Collins, W.D., Friedlingstein, P., Gaye, A.T., Gregory, J.M., Kitoh, A., Knutti, R., Murphy, J.M., Noda, A., Raper, S.C.B., Watterson, I.G., Weaver, A.J., Zhao, Z.C., 2007. Global climate projections. In: Solomon, S., Qin, D., Manning, M., Chen, Z., Marquis, M., Averyt, K.B., Tignor, M., Miller, H.L. (Eds.), *Climate Change 2007: The Physical Science Basis. Contribution of Working Group I to the Fourth Assessment Report to the Intergovernmental Panel on Climate Change*. Cambridge University Press, Cambridge, United Kingdom and New York, NY, USA.
- Mills, G., Buse, A., Gimeno, B., Bermejo, V., Holland, M., Emberson, L., Pleijel, H., 2007. A synthesis of AOT40-based response functions and critical levels of ozone for agricultural and horticultural crops. *Atmos. Environ.* 41, 2630–2643.
- Mills, G., Hayes, F., Simpson, D., Emberson, L., Norris, D., Harmens, H., Buker, P., 2011a. Evidence of widespread effects of ozone on crops and (semi-)natural vegetation in Europe (1990–2006) in relation to AOT40 and flux-based risk maps. *Glob. Change Biol.* 17, 592–613.
- Mills, G., Pleijel, H., Braun, S., Buker, P., Bermejo, V., Calvo, E., Danielsson, H., Emberson, L., Fernandez, I.G., Grunhage, L., Harmens, H., Hayes, F., Karlsson, P.E., Simpson, D., 2011b. New stomatal flux-based critical levels for ozone effects on vegetation. *Atmos. Environ.* 45, 5064–5068.
- Mittler, R., 2006. Abiotic stress, the field environment and stress combination. *Trends Plant Sci.* 11, 15–19.
- Morris, M.D., 1991. Factorial sampling plans for preliminary computational experiments. *Technometrics* 33, 161–174.
- Nie, G.Y., Tomasevic, M., Baker, N.R., 1993. Effects of ozone on the photosynthetic apparatus and leaf proteins during leaf development in wheat. *Plant Cell Environ.* 16, 643–651.
- Ollerenshaw, J.H., Lyons, T., 1999. Impacts of ozone on the growth and yield of field-grown winter wheat. *Environ. Pollut.* 106, 67–72.
- Pickering, N.B., Hansen, J.W., Jones, J.W., Wells, C.M., Chan, V.K., Godwin, D.C., 1994. WeatherMan: a utility for managing and generating daily weather data. *Agron. J.* 86, 332–337.
- Pleijel, H., Broberg, M.C., Uddling, J., Mills, G., 2018. Current surface ozone concentrations significantly decrease wheat growth, yield and quality. *Sci. Total Environ.* 613, 687–692.
- Porter, J.R., 1993. AFRWHEAT2: a model of the growth and development of wheat incorporating responses to water and nitrogen. *Eur. J. Agron.* 2, 69–82.
- Reyenga, P.J., Howden, S.M., Meinke, H., McKeon, G.M., 1999. Modelling global change impacts on wheat cropping in south-east Queensland, Australia. *Environ. Modell. Softw.* 14, 297–306.
- Roche, D., 2015. Stomatal conductance is essential for higher yield potential of C-3 crops. *Crit. Rev. Plant Sci.* 34, 429–453.
- Semenov, M.A., Shewry, P.R., 2011. Modelling predicts that heat stress, not drought, will increase vulnerability of wheat in Europe. *Sci. Rep.* 1, 5.
- Sheffield, J., Wood, E.F., 2008. Projected changes in drought occurrence under future global warming from multi-model, multi-scenario, IPCC AR4 simulations. *Clim. Dyn.* 31, 79–105.
- Shiferaw, B., Smale, M., Braun, H.J., Duveiller, E., Reynolds, M., Muricho, G., 2013. Crops that feed the world 10. Past successes and future challenges to the role played by wheat in global food security. *Food Secur.* 5, 291–317.
- Sicard, P., Anav, A., De Marco, A., Paoletti, E., 2017. Projected global ground-level ozone impacts on vegetation under different emission and climate scenarios. *Atmos. Chem. Phys.* 17, 12177–12196.
- Simpson, D., Arneth, A., Mills, G., Solberg, S., Uddling, J., 2014. Ozone - the persistent menace: interactions with the N cycle and climate change. *Curr. Opin. Environ. Sustain.* 9–10, 9–19.
- Soil Survey Staff, 2018. Natural Resources Conservation Service. United States Department of Agriculture Web Soil Survey.
- Spitters, C.J.T., Schapendonk, A., 1990. Evaluation of breeding strategies for drought tolerance in potato by means of crop growth simulation. *Plant Soil* 123, 193–203.
- Tao, F.L., Feng, Z.Z., Tang, H.Y., Chen, Y., Kobayashi, K., 2017. Effects of climate change, CO₂ and O₃ on wheat productivity in Eastern China, singly and in combination. *Atmos. Environ.* 153, 182–193.

- Tester, M., Bacic, A., 2005. Abiotic stress tolerance in grasses. From model plants to crop plants. *Plant Physiol.* 137, 791–793.
- Trnka, M., Rotter, R.P., Ruiz-Ramos, M., Kersebaum, K.C., Olesen, J.E., Zalud, Z., Semenov, M.A., 2014. Adverse weather conditions for European wheat production will become more frequent with climate change. *Nat. Clim. Chang.* 4, 637–643.
- U.S. EPA, 2006. Air Quality Criteria for Ozone and Related Photochemical Oxidants (Final Report, 2006). U.S. Environmental Protection Agency, Washington, DC.
- USDA-NASS, 2017. United States Department of Agriculture (USDA) - National Agriculture Statistics Service (NASS) Quick Stats Tool.
- Vainonen, J.P., Kangasjarvi, J., 2015. Plant signalling in acute ozone exposure. *Plant Cell Environ.* 38, 240–252.
- Van Dingenen, R., Dentener, F.J., Raes, F., Krol, M.C., Emberson, L., Cofala, J., 2009. The global impact of ozone on agricultural crop yields under current and future air quality legislation. *Atmos. Environ.* 43, 604–618.
- Vingarzan, R., 2004. A review of surface ozone background levels and trends. *Atmos. Environ.* 38, 3431–3442.
- Wang, X.P., Mauzerall, D.L., 2004. Characterizing distributions of surface ozone and its impact on grain production in China, Japan and South Korea: 1990 and 2020. *Atmos. Environ.* 38, 4383–4402.
- Wehner, M., Easterling, D.R., Lawrimore, J.H., Heim, R.R., Vose, R.S., Santer, B.D., 2011. Projections of future drought in the Continental United States and Mexico. *J. Hydrometeorol.* 12, 1359–1377.
- Wild, O., Fiore, A.M., Shindell, D.T., Doherty, R.M., Collins, W.J., Dentener, F.J., Schultz, M.G., Gong, S., MacKenzie, I.A., Zeng, G., Hess, P., Duncan, B.N., Bergmann, D.J., Szopa, S., Jonson, J.E., Keating, T.J., Zuber, A., 2012. Modelling future changes in surface ozone: a parameterized approach. *Atmos. Chem. Phys.* 12, 2037–2054.
- Zhang, Y.Z., Wang, Y.H., 2016. Climate-driven ground-level ozone extreme in the fall over the Southeast United States. *Proc. Natl. Acad. Sci. U. S. A.* 113, 10025–10030.